Excited-state proton transfer relieves antiaromaticity in molecules

Chia-Hua Wu[a], Lucas José Karas[a], Henrik Ottosson[b], and Judy I-Chia Wu[a,1]

[a]Department of Chemistry, University of Houston, Houston, TX 77004; and [b]Department of Chemistry, Ångström Laboratory, Uppsala University, 751 20 Uppsala, Sweden

Edited by Kendall N. Houk, University of California, Los Angeles, CA, and approved August 28, 2019 (received for review May 20, 2019)

Baird's rule explains why and when excited-state proton transfer (ESPT) reactions happen in organic compounds. Bifunctional compounds that are [4*n* + 2] π-aromatic in the ground state, become [4*n* + 2] π-antiaromatic in the first $^1\pi\pi^*$ states, and proton transfer (either inter- or intramolecularly) helps relieve excited-state antiaromaticity. Computed nucleus-independent chemical shifts (NICS) for several ESPT examples (including excited-state intramolecular proton transfers (ESIPT), biprotonic transfers, dynamic catalyzed transfers, and proton relay transfers) document the important role of excited-state antiaromaticity. *o*-Salicylic acid undergoes ESPT only in the "antiaromatic" S_1 ($^1\pi\pi^*$) state, but not in the "aromatic" S_2 ($^1\pi\pi^*$) state. Stokes' shifts of structurally related compounds [e.g., derivatives of 2-(2-hydroxyphenyl)benzoxazole and hydrogen-bonded complexes of 2-aminopyridine with protic substrates] vary depending on the antiaromaticity of the photoinduced tautomers. Remarkably, Baird's rule predicts the effect of light on hydrogen bond strengths; hydrogen bonds that enhance (and reduce) excited-state antiaromaticity in compounds become weakened (and strengthened) upon photoexcitation.

excited-state proton transfer | Baird's rule | aromaticity | antiaromaticity | hydrogen bonding

When light strikes a molecule, protons and electrons can sometimes rearrange to form rare tautomers in ratios far from equilibrium. Weller discovered the first example of such excited-state proton transfer (ESPT) in the *o*-salicylic acid—a large Stokes' shift in the spectrum suggested the appearance of an odd tautomer (1, 2). At first, Weller and others (3) assumed that a zwitterionic tautomer had formed, but Nagaoka et al. (4, 5) later proposed that an H atom migrated from the hydroxyl to the carboxyl group, giving a quinoid-looking tautomer (Fig. 1*A*, **Q** form). Similar prominent Stokes' shifts (up to 10,000 cm^{-1}) and astonishing proton transfer rates (up to 10^{12} s^{-1}) were reported for the dimers of 7-azaindole (6, 7), 1-carbazole (8, 9), and protic solvent complexes of 2-aminopyridine (10–12), and even more reported examples of ESPT in organic compounds emerged in the next 30 y (13). Compounds like the 3-hydroxyflavone (14, 15), 2-(2-hydroxyphenyl)benzoxazole (HBO) (16), and 10-hydroxybenzo[*h*]quinolone (HBQ) (17) undergo excited-state intramolecular proton transfer (ESIPT) (18, 19) at the picosecond scale, display large Stokes' shifts, and find myriad applications as dyes and fluorescent sensors. When ESPT happens, only bare protons are displaced, but what prompts them to move is enormous change in the electronic structure of the molecule. Chemists have called this change "an increase in the acidity of the proton donor and basicity of the proton acceptor (pK_a change)," (19, 20) "a difference in the character of the wavefunction (Nagaoka's nodal plane model)," (4, 5) or "a change in aromatic character." (21–24) In this paper, we show that when an organic compound is: cyclic, π-conjugated, and exhibits prominent [4*n* + 2] π-aromatic character in the ground state, that change is the rise of [4*n* + 2] π-antiaromaticity in its photoexcited state.

Baird first proposed a set of rules describing that the Hückel π-electron counting rules of aromaticity and antiaromaticity reverse at the lowest $\pi\pi^*$ triplet state (25). In the ground state, compounds with cyclic [4*n* + 2] π-electron delocalizations display enhanced thermochemical stability, have low reactivity, and are aromatic. Those with [4*n*] π-electron delocalizations are less viable, chemically reactive, and are antiaromatic. In the excited state, the opposite is true (26–29). Compounds with cyclic [4*n*] π-electron delocalizations become aromatic; those with [4*n* + 2] π-electron delocalizations become antiaromatic. It was suggested that Baird's rule extends also to the lowest $\pi\pi^*$ singlet states (26, 28, 29), to macrocycles (30, 31), and that the concept has much interpretive merit for photochemistry (32, 33). Benzene, for example, is [4*n* + 2] π-electron antiaromatic in its lowest $^1\pi\pi^*$ and $^3\pi\pi^*$ states (34); it becomes highly reactive and does what it can to relieve excited-state antiaromaticity. We show here that bifunctional molecules, i.e., compounds that have both proton donating and accepting groups, like the *o*-salicylic acid, can relieve excited-state antiaromaticity through ESPT. In the ground state, the dominant tautomer of *o*-salicylic acid (Fig. 1*A*, **A** form) is aromatic and displays a cyclic delocalization of [4*n* + 2] π-electrons. But this tautomeric form becomes antiaromatic in the first $^1\pi\pi^*$ state, and one way for it to get rid of antiaromaticity is to transfer a proton from the hydroxyl to the carboxyl group, and form **Q**—a quinoidal tautomer preclude of cyclic [4*n* + 2] π-electron delocalization. In this way, ESPT can relieve excited-state antiaromaticity in cyclic, π-conjugated, bifunctional compounds.

Depending on how a migrating proton moves from one site to another, ESPT reactions are categorized into 4 types (35): ESIPT (type I), biprotonic transfers (type II), dynamic catalyzed proton

Significance

Excited-state proton transfer (ESPT) is universally recognized as a reaction that relaxes the energy of a photoexcited organic compound. It is commonly found in many light-driven processes. Here we identify decisive principles underlying why and when ESPT happens. Our computational investigation of prototypical ESPT reactions finds that the occurrence of ESPT can be explained by an electron-counting rule—Baird's rule, which remains largely ignored despite having a near–50-y-old history. We emphasize that this surprising connection not only explains the mechanistic principle of ESPT reactions, but it also predicts whether hydrogen bonding interactions that form within and between organic compounds might strengthen or weaken when irradiated by light. Recognizing this relationship has tremendous interpretive merit for organic photochemistry.

Author contributions: C.-H.W. and J.I.W. designed research; C.-H.W. and L.J.K. performed research; C.-H.W., L.J.K., H.O., and J.I.W. analyzed data and made intellectual contributions to the development of the paper; and J.I.W. wrote the paper.

The authors declare no conflict of interest.

This article is a PNAS Direct Submission.

[1]To whom correspondence may be addressed. Email: jiwu@central.uh.edu.

This article contains supporting information online at www.pnas.org/lookup/suppl/doi:10.1073/pnas.1908516116/-/DCSupplemental.

First Published September 25, 2019.

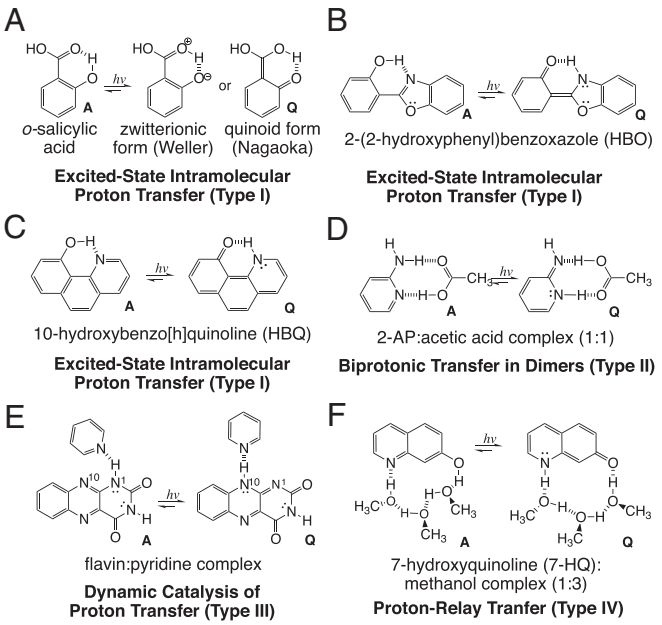

Fig. 1. Examples of type I (*A–C*), type II (*D*), type III (*E*), and type IV (*F*) ESPT reactions. Tautomers having complete cyclic [4*n* + 2] π-electron delocalizations are labeled "**A**." Tautomers having breached cyclic π-electron delocalizations are labeled "**Q**."

transfers (type III), and proton relay transfers involving multiple proton bridges (type IV). In dynamic catalyzed proton transfers, the catalyzing substrate shifts its position during ESPT. For example, flavin, a photoactive cofactor in enzymes, can form 1:1 complexes with pyridine and undergo dynamic catalyzed ESPT; pyridine extracts a proton from the N_1 site of flavin and rotates its position to donate that same proton to the N_{10} site (Fig. 1*E*) (36, 37). In proton relay transfer reactions, for example, in 7-hydroxyquinoline (7-HQ), a proton can migrate from the hydroxyl site to the N site through a chain of methanol or ammonia solvent (Fig. 1*F*) (38, 39). Selected examples of these ESPT types are shown in Fig. 1.

Notably, all of the compounds, shown in Fig. 1 and known to undergo ESPT, are [4*n* + 2] π-aromatic in the ground state (see **A** forms), but become [4*n* + 2] π-antiaromatic when promoted to the first ππ* state. The **A** forms of both *o*-salicylic acid and 2-aminopyridine (2-AP) exhibit cyclic delocalized 6 π-electrons in the ring (Fig. 1 *A* and *D*). In HBO, a cyclic 6 π-electron delocalized benzenoid ring is joined through a single C–C bond to a cyclic 10 π-electron delocalized benzoxazole (Fig. 1*B*). In HBQ, the aza-phenanthrene skeleton exhibits 14-ring π-electrons (Fig. 1*C*). Both flavin and 7-HQ have aza-naphthalene moieties with 10-ring π-electrons (Fig. 1 *E* and *F*). Here, we show that ESPT helps to relieve excited-state antiaromaticity in all of these cyclic [4*n* + 2] π-electron systems. In relation to the recognized role of excited-state antiaromaticity in ESPT, we also demonstrate that Baird's rule can be used to explain and predict the effects of photoexcitation on hydrogen bond strengths.

Results and Discussion

Relief of Excited-State Antiaromaticity in ESPT Reactions. Computed tautomerization energies (ΔE_T) of the S_0, S_1, and T_1 states of *o*-salicylic acid, HBO, HBQ, the 1:1 complex of 2-AP:acetic acid, the flavin:pyridine complex, and the 1:3 complex of 7-HQ:methanol (values in bold, in Table 1) show that, in the S_0 state, the **A** forms (i.e., tautomers with cyclic [4*n* + 2] π-electron delocalizations) are consistently lower in energy than the **Q** forms. But, in the S_1 (^{1}ππ*) and T_1 (^{3}ππ*) states, the **Q** forms (i.e., tautomers with "breached" π-electron delocalizations) become energetically competitive. Tautomeric free energies computed in implicit solvation at 298 K are provided in *SI Appendix*, Table S1, and show the same trend. Unless noted otherwise, all S_1 states refer to ^{1}ππ* states and all T_1 states refer to ^{3}ππ* states (for comparison, transition energies for the closest energy ^{1}nπ* states are provided in *SI Appendix*, Tables S2 and S3).

Dissected nucleus-independent chemical shifts (40, 41), $NICS(1)_{zz}$, analyses suggest that the tautomeric trends shown in Table 1 are the result of reversed aromaticity vs. antiaromaticity in **A**, in the S_0 vs. S_1 (and T_1) states. In the S_0 state, the computed $NICS(1)_{zz}$ values for all **A** forms are large and negative, indicating strong aromatic character. But, in the S_1 (and T_1) state, these values become large and positive, indicating strong antiaromatic character. In contrast, the **Q** forms display less-negative $NICS(1)_{zz}$ values in the S_0 state, and less-positive $NICS(1)_{zz}$ values [modestly negative $NICS(1)_{zz}$ value for HBO] in the S_1 (and T_1) states. Direct comparisons of computed $NICS(1)_{zz}$ values for the **A** vs. **Q** tautomers, in the S_1 (and T_1) state, suggest that ESPT helps to relieve excited-state antiaromaticity. Computed Harmonic Oscillator Model of Electron Delocalization analyses (a geometric criterion of aromaticity and antiaromaticity) are supportive and show the same trends (see results in *SI Appendix*, Tables S5–S8). Similar findings have been reported for ESIPT compounds, based on magnetic (42), geometric (21, 23), and energetic (24) indices of aromaticity.

Remarkably, Baird's rule helps to explain when and why π-conjugated organic compounds undergo ESPT. Below we elucidate the important role of Baird's rule for explaining the mechanisms of: 1) ESIPT, 2) solvent-catalyzed phototautomerizations, as well as 3) the effects of photoexcitation on hydrogen bond strengths.

ESIPT reactions. ESIPT in systems like the *o*-salicylic acid, HBO, and HBQ, (Fig. 1 *A–C*), have been viewed as a consequence of "a redistribution of electron density," "a change in acidity and basicity," or "a change in the wavefunction," in molecules at photoexcited states. We show here that these interpretations differ in choice of words but describe the same phenomena—they capture the rise of antiaromaticity in photoexcited molecules. Relief of antiaromaticity in ESIPT molecules helps to explain: 1) when ESIPT happens and when it does not (e.g., in different electronic states of *o*-salicylic acid), and 2) why structurally related molecules can exhibit surprisingly different Stokes' shifts (e.g., in analogs of HBO).

In *o*-salicylic acid, ESIPT happens only in the S_1 state, but not in the S_2 (^{1}ππ*) state (the closest energy ^{1}nπ* state has a 0.04 eV higher transition energy). This follows a proposed sequence of electron-counting rules for aromaticity and antiaromaticity in molecules in the S_0, S_1, and S_2 ππ* states (43). It was suggested that "Hückel aromatic rings with [4*n* + 2] π-electrons become antiaromatic in the first singlet excited state and switch back to aromatic in the second singlet excited state." (43) Computed $NICS(1)_{zz}$ values for *o*-salicylic acid in the S_0 (**A**: –21.9 ppm), S_1 ^{1}ππ* (**A**: +64.5 ppm), and S_2 ^{1}ππ* (**A**: –72.4 ppm, see details in *SI Appendix*, Table S9) states document this "switch," showing strong aromatic character in the **A** form of *o*-salicylic acid in the S_2 state. In the S_1 state, ESIPT to the **Q** form reduces antiaromatic character in the 6-membered ring (**Q**: +18.2 ppm) (Fig. 2*A*). No ESIPT reaction occurs in the S_2 state of *o*-salicylic acid, since there is no need to relieve any antiaromaticity. Whether or not ESIPT happens in a photoexcited molecule largely depends on the (anti)aromatic character of the electronic state considered.

Structurally related ESIPT molecules can display surprisingly different Stokes' shifts, depending on their (anti)aromatic characters. For example, the **Q** forms of 2 benzo-fused HBO analogs, 1H2NBO and 2H3NBO (Fig. 2 *B* and *C*), are known to exhibit very different emission wavelengths (470 vs. 670 nm) in hexane solution (44). Computed $\Delta NICS(1)_{zz}$ ($S_1 - S_0$) for $1H2NBO_{(\mathbf{Q})}$ (Δ = 71.2 ppm) and $2H2NBO_{(\mathbf{Q})}$ (Δ = 63.7 ppm) indicate that S_1

Table 1. Computed NICS(1)$_{zz}$ values (in ppm) and tautomerization energies (ΔE_T, in kcal/mol) for A and Q forms in the S_0, S_1, and T_1 states

	NICS(1)$_{zz}$ (in ppm), ΔE_T values (in kcal/mol)		
Systems	S_0	S_1 approx.	T_1
o-Salicylic acid			
(A)	−21.9	+64.5	+47.4
(Q)	−11.1*	+18.2	+10.9
ΔE_T	**[+19.8]***	**−0.1**	**−4.8**
HBO			
(A)	−66.6 (−20.8, −18.1, −27.7)†	+28.2 (+26.4, +0.0, +1.8)†	+17.5 (+14.3, +0.9, +2.3)†
(Q)	−52.3 (−12.5, −13.1, −26.7)†	−5.3 (+12.2, −2.7, −14.8)†	−10.2 (+9.0, −2.9, −16.3)†
ΔE_T	**+12.3**	**−4.5**	**−4.2**
1H2NBO			
(A)	−90.4 (−26.2, −19.4, −17.4, −27.4)†	+30.8 (+21.5, +35.9, −11.0, −15.6)†	+17.2 (+16.6, +31.1, −12.4, −18.1)†
(Q)	−69.2 (−25.2, −7.3, −10.9, −25.8)†	+2.0 (+5.8, +12.3, −2.9, −13.2)†	−5.9 (+2.2, +8.6, −2.5, −14.2)†
ΔE_T	**+7.9**	**+0.9**	**+1.9**
2H3NBO			
(A)	−91.3 (−23.9, −22.3, −17.6, −27.5)†	+57.1 (+38.2, +56.8, −15.1, −22.8)†	+18.2 (+21.7, +38.2, −16.9, −24.8)†
(Q)	−73.5 (−15.7, −16.7, −14.0, −27.1)†	−9.8 (−0.1, +16.5, −5.8, −20.4)†	−16.8 (−3.8, +14.4, −6.1, −21.3)†
ΔE_T	**[+15.6]***	**−6.5**	**−5.1**
HBQ			
(A)	−73.1 (−27.7, −17.9, −27.6)†	+232.7 (+83.5, +60.4, +88.8)*, †	+117.4 (+42.3, +34.1, +40.9)†
(Q)	−56.2 (−23.8, −12.4, −20.0)*, †	+88.3 (+24.3, +9.8, +54.1)[b]	+67.3 (+19.3, +5.0, +43.0)†
ΔE_T	**[+13.6]***	**[−10.0]***	**−12.7**
2-AP:acetic acid (1:1)			
(A)	−17.9	+84.3	+54.4
(Q)	−7.4	+33.4	+28.5
ΔE_T	**+8.7**	**−5.7**	**−7.2**
Flavin:pyridine (1:1)			
(A)	−47.3 (−26.0, −22.4, +1.1)†	+90.3 (+41.7, +47.7, +0.9)†	+65.6 (+30.2, +34.8, +0.6)†
(Q)	−30.6 (−23.3, −8.1, +0.8)†	+28.3 (+7.3, +19.9, +1.1)†	+28.2 (+7.4, +19.9, +0.9)†
ΔE_T	**+10.7**	**+1.1**	**+1.9**
7-HQ:methanol wire (1:3)			
(A)	−48.9 (−24.2, −24.7)†	+152.9 (+72.2, +80.7)†	+74.2 (+30.4, +43.8)†
(Q)	−29.9 (−12.9, −17.0)†	+71.2 (+45.5, +25.7)†	+48.0 (+28.9, +19.1)†
ΔE_T	**+7.8**	**−14.4**	**−10.9**

NICS(1)$_{zz}$ values were computed at PW91/IGLOIII//(TD-)ωB97X-D/6–311+G(d,p). When multiple rings are present, a sum of all NICS(1)$_{zz}$ values is presented (values for individual rings are shown in parentheses). Tautomeric energies (ΔE_T, in kcal/mol), in bold, were computed at (TD-)ωB97X-D/6–311+G(d,p). Positive ΔE_T values indicate a higher-energy **Q** form ($\Delta E_T = E_{(Q)} - E_{(A)}$)

*Hydrogen-bonding O–H bond fixed to 0.96 Å and N–H bond fixed to 1.00 Å. Values in brackets are based on comparisons to nonminima **A** or **Q** form structures with fixed hydrogen bonding O–H or N–H bonds.

†NICS values for individual rings, from left to right, as shown in Fig. 1.

to S_0 emission relieves more antiaromaticity in 1H2NBO$_{(Q)}$ than in the (modestly aromatic) 2H3NBO$_{(Q)}$ (Table 1). Note the presence of 2 Clar sextets in 1H2NBO$_{(Q)}$ (both antiaromatic at S_1, and both aromatic at S_0), but only one in 2H3NBO$_{(Q)}$ (Fig. 2). In 1H2NBO$_{(Q)}$, the larger ΔNICS(1)$_{zz}$ value reflects a larger energy gap between the S_1 and S_0 states (83.1 kcal/mol), corresponding to a shorter emission wavelength. In 2H3NBO$_{(Q)}$, the smaller ΔNICS(1)$_{zz}$ value reflects a smaller energy gap between the S_1 and S_0 states (56.4 kcal/mol), corresponding to a longer emission wavelength. In this way, the expected emissions of tautomers arising from ESIPT can be related to their inherent (anti)aromatic characters. See T_1 state results in *SI Appendix*, Table S13. A recent experimental paper reported similar findings for other derivatives of HBO (42). Together these evidence (21, 23, 24, 42) suggest that the π-conjugation patterns of ESIPT compounds may be designed to tune the magnitude of their Stokes' shifts.

Solvent-catalyzed phototautomerizations. Solvent-catalyzed phototautomerization of 2-AP is a classic example of ESPT (Fig. 1*D*). It was shown that, upon photoexcitation, protic solvents like acetic acid, propionic acid, and formic acid catalyzed the tautomerization of 2-AP$_{(A)}$→2-AP$_{(Q)}$ through double proton transfer (10, 11). Even though tautomeric forms with higher polarity are typically preferred in polar solvents, the relative stabilities of 2-AP$_{(A)}$ and 2-AP$_{(Q)}$ in these protic solvents are in the reversed order. In the ground state, the less-polar 2-AP$_{(A)}$ (computed dipole moment: 2.03 μ vs. 2.97 μ for 2-AP$_{(Q)}$) dominates (the experimental dipole moment of 2-AP$_{(A)}$ is 2.06 μ) (45). In the S_1 state, the less-polar 2-AP$_{(Q)}$ (0.98 μ vs. 3.21 μ for 2-AP$_{(A)}$) dominates. It was proposed that the effects of ESPT in the 2-AP:acetic acid complex may be explained by increased basicity of the ring N in 2-AP upon photoexcitation (12); fluorescence experiments showed an increase in pK_a from 6.86 to 8.95 (46). Here, we show that changes in the photoacidity and photobasicity of the proton donor and proton acceptor sites of 2-AP are the result of emerging excited-state antiaromaticity in the 2-AP ring. Although the hydrogen bonds and migrating protons are not part of the aromatic core of the chromophore, they are directly linked to changes in the electronic structure of the π-conjugated ring upon photoexcitation.

Results based on the 1:1 complex of 2-AP:acetic acid show that, in the S_0 state, 2-AP$_{(A)}$:acetic acid is 8.6 kcal/mol lower in energy than 2-AP$_{(Q)}$:acetic acid, and double proton transfer, going through a transition state structure (**TS**), is endothermic. Computed NICS(1)$_{zz}$ values at these stationary points show decreasing

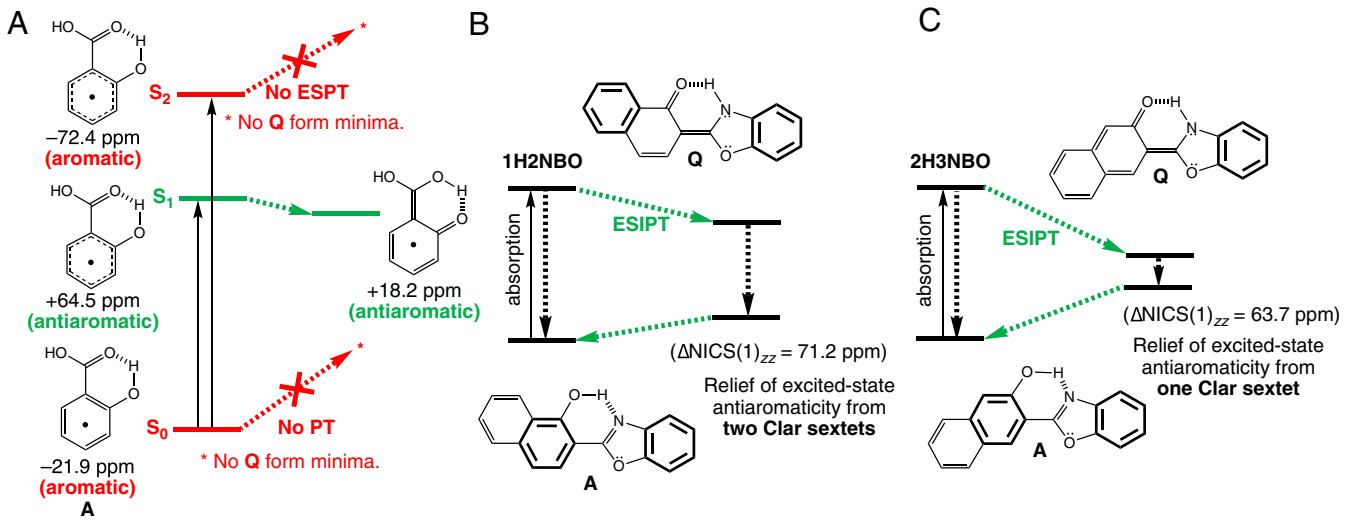

Fig. 2. (*A*) Computed NICS(1)$_{zz}$ values show that the dominant **A** form tautomer of *o*-salicylic acid is aromatic at S_0 (no proton transfer), antiaromatic at S_1 (ESIPT occurs), and aromatic at S_2 (no ESIPT). Schematic illustrations of ESIPT in (*B*) 1H2NBO and (*C*) 2H3NBO adapted from ref. 19. Clar sextets in the **A** and **Q** forms of both structures are highlighted in bold.

negative NICS values **A** (−17.9 ppm) → **TS** (−9.7 ppm) → **Q** (−7.4 ppm) (*SI Appendix*), indicating loss of aromaticity upon double proton transfer. In the first ππ* states, the opposite happens. In the S_1 state, 2-AP$_{(A)}$:acetic acid is 5.7 kcal/mol higher in energy than 2-AP$_{(Q)}$:acetic acid. Double proton transfer is near barrierless and exothermic. Computed NICS(1)$_{zz}$ values at the relevant stationary points show decreasing positive NICS values **A** (+84.3 ppm) → **TS** (+65.4 ppm) → **Q** (+33.4 ppm), indicating loss of antiaromaticity in the 2-AP ring upon ESPT. Computations in the T_1 state also show decreasing positive NICS values going from **A** (+54.4ppm) → **TS** (+48.2 ppm) → **Q** (+28.5ppm).

Based on a survey of 10 1:1 complexes of 2-AP:substrate (protic substrates considered include: acetic acid **1**, methanol **2**, *t*-butanol **3**, water **4**, aza-enamine **5**, guanidine **6**, formamide **7**, ammonia **8**, a zwitterionic glycine **9**, and glycine **10**), excellent linear correlation was found between the computed ΔNICS(1)$_{zz}$ ($S_1 - S_0$) values for 2-AP$_{(Q)}$ vs. the estimated S_1 emission wavelengths of 2-AP$_{(Q)}$ (r = 0.953) (Fig. 3*B*). Shorter emission wavelengths correspond to hydrogen-bonded 2-AP$_{(Q)}$ rings with stronger ground-state aromaticity (i.e., a more stabilized S_0 state) and stronger excited-state antiaromaticity (i.e., a more destabilized S_1 state). Longer emission wavelengths correspond to hydrogen-bonded 2-AP$_{(Q)}$ rings with weaker ground-state aromaticity (i.e., a less-stabilized S_0 state) and weaker excited-state antiaromaticity (i.e., a less-destabilized S_1 state). Results computed in the T_1 states also show excellent correlation for the computed ΔNICS(1)$_{zz}$ ($T_1 - S_0$) values vs. emission wavelengths of 2-AP$_{(Q)}$ (r = 0.997) (*SI Appendix*). Importantly, hydrogen-bonding substrates can influence the spectroscopic signatures of ESPT compounds by modifying the ground- and excited-state (anti)aromaticity of the photoinduced tautomer. Solvent effects on the Stokes' shifts of ESPT processes may be explained similarly.

Predicting the effects of photoexcitation on hydrogen bond strengths. Despite long-standing interests in applying excited-state hydrogen bonds as design components of functional molecules and materials, there is currently no a priori way to predict if the strike of a light pulse will strengthen or weaken a hydrogen bond. We show here that the effects of photoexcitation on hydrogen bond strengths depend on the π-conjugation patterns of the hydrogen-bonding compounds. At photoexcited states, hydrogen bonds that help decrease excited-state antiaromaticity in molecules become stronger; those that increase excited-state antiaromaticity in molecules become weaker.

Results based on the hydrogen-bonded dimer of 2-AP are discussed below. It was suggested that, in the excited state, the 2-AP dimer undergoes electron transfer followed by immediate proton transfer (47). Here the 2-AP dimer is considered as a theoretical model. Both 2-AP$_{(A)}$ dimer and 2-AP$_{(Q)}$ dimer exhibit 2 sets of N–H. . .N hydrogen bonds, but photoexcitation changes their strengths in opposite directions. Computed interaction energies (ΔE_{int}) for the singlet (S_0), triplet (T_1), and quintuplet (Q_1) states of the 2-AP$_{(Q)}$ dimer suggest that the 2 sets of N–H. . .N hydrogen bonds become increasingly strong when one and both fragments are promoted to the T_1 ππ* state: S_0 dimer (ΔE_{int} = −11.6 kcal/mol, S_0 monomer + S_0 monomer), T_1 dimer (−14.5 kcal/mol, S_0 monomer + T_1 monomer), Q_1 dimer (−18.7 kcal/mol, T_1 monomer + T_1 monomer). Conversely, computed ΔE_{int} values for the 2-AP$_{(Q)}$ dimer indicate that the 2 sets of N–H. . .H hydrogen bonds become increasingly weak when one and both fragments are promoted to the T_1 ππ* state: S_0 dimer (ΔE_{int} = −22.9 kcal/mol, S_0 + S_0), T_1 dimer (−17.3 kcal/mol, T_1 + S_0), Q_1 dimer (−13.3 kcal/mol, T_1 + T_1).

Photoexcitation strengthens the hydrogen bonds of 2-AP$_{(A)}$ dimer (Fig. 4*A*) but weakens those of 2-AP$_{(Q)}$ dimer (Fig. 4*B*), due to changes in ground- and excited-state (anti)aromaticity. In the 2-AP$_{(A)}$ dimer, the 2 hydrogen bonds polarize the π-electrons of

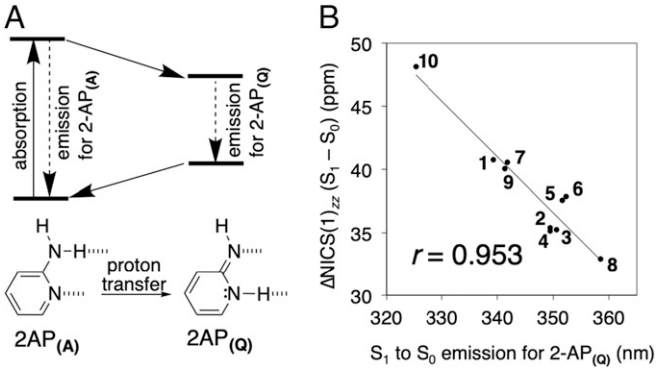

Fig. 3. (*A*) Illustration of ESPT in 1:1 complexes of 2-AP:substrate (substrates: **1–10**). Plot of computed (*B*) ΔNICS(1)$_{zz}$ ($S_1 - S_0$) vs. emission wavelengths for 2-AP$_{(Q)}$:substrate complexes.

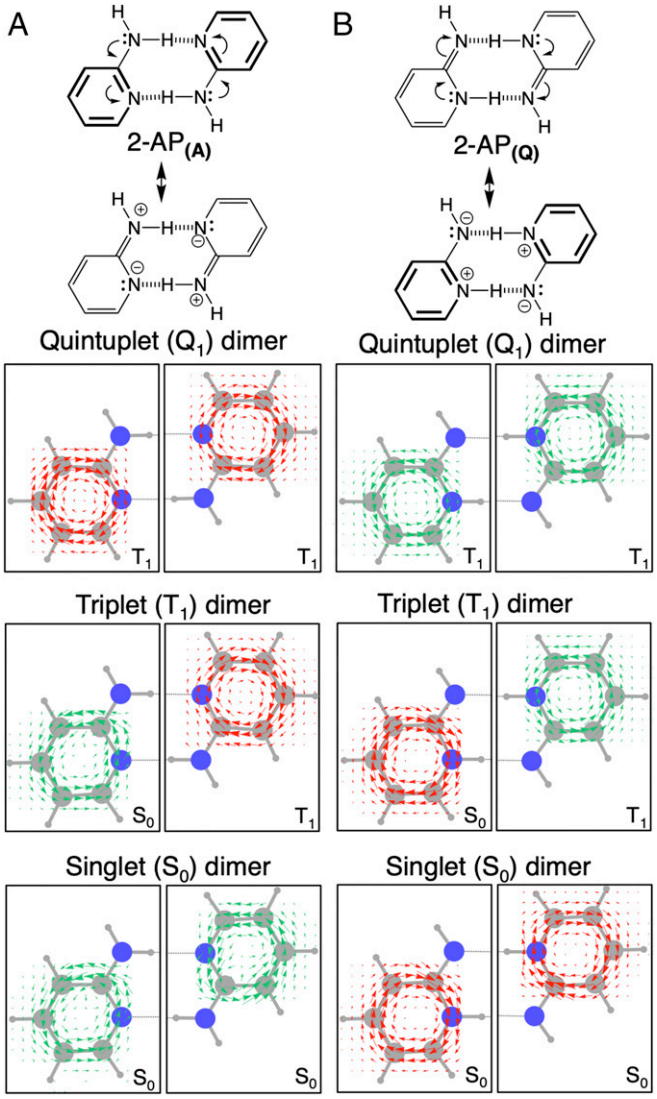

Fig. 4. ΔGIMIC plots computed at 1 Å above the ring plane for (*A*) 2-AP$_{(A)}$ dimer and (*B*) 2-AP$_{(Q)}$ dimer, at the S_0 ($S_0 + S_0$), T_1 ($S_0 + T_1$), and Q_1 ($T_1 + T_1$) states. Green "anticlockwise" currents indicate increased paratropicity (or decreased diatropicity) upon hydrogen bonding. Red "clockwise" currents indicate decreased paratropicity (or increased diatropicity) upon dimerization.

2-AP$_{(A)}$ and reduce cyclic [$4n + 2$] π-electron delocalization in both rings (see resonance form with breached π-conjugation in Fig. 4 *A*, *Left*). In the ground state, this polarization effect weakens aromaticity in the 6-membered ring. In the T_1 state, this effect weakens antiaromaticity, and the corresponding photoexcited hydrogen bonds are strengthened. The opposite happens in the 2-AP$_{(Q)}$ dimer. In the 2-AP$_{(Q)}$ dimer, the 2 hydrogen bonds polarize the π-electrons of 2-AP$_{(Q)}$ and enhance cyclic [$4n + 2$] π-electron delocalization in both rings (see resonance form with cyclic delocalized 6 π-electrons in Fig. 4 *B*, *Right*). In the ground state, this polarization effect strengthens aromaticity in the 6-membered ring. In the T_1 state, this effect strengthens antiaromaticity, and the corresponding photoexcited hydrogen bonds are weakened.

Computed NICS(1)$_{zz}$ (Table 2) and difference plots of gauge-included magnetically induced currents (48) (ΔGIMIC) (Fig. 4) document the effects described above. Clockwise current plots (in red) indicate aromaticity gain or antiaromaticity loss upon hydrogen bonding. Anticlockwise current plots (in green) indicate aromaticity loss or antiaromaticity gain upon hydrogen bonding. In the S_0 state of 2-AP$_{(A)}$ dimer, hydrogen bonding decreases aromaticity in both 2-AP$_{(A)}$ rings (Fig. 4 *A*, *Bottom*). In the T_1 state, hydrogen bonding decreases aromaticity in one 2-AP$_{(A)}$ ring but decreases antiaromaticity in the other (Fig. 4 *A*, *Middle*). In the Q_1 state, hydrogen bonding decreases excited-state antiaromaticity in both 2-AP$_{(A)}$ rings (Fig. 4 *A*, *Top*). These effects are opposite in the 2-AP$_{(Q)}$ dimer (Fig. 4*B*). In this way, Baird's rule may be applied to control and predict the effects of photoexcitation on hydrogen bonding.

Table 2. Computed NICS(1)$_{zz}$ values for the A and Q forms of 2-AP and 2-AP dimer

Systems	NICS(1)$_{zz}$ (in ppm)		
	S_0	T_1	Q_1
2-AP$_{(A)}$	−20.5	+55.0	N/A
2-AP$_{(A)}$ dimer	−18.0, −18.0	−17.8, +53.7	+52.2, +52.2
2-AP$_{(Q)}$	−2.5	+20.8	N/A
2-AP$_{(Q)}$ dimer	−6.6, −6.6	−5.6, +28.0	+26.7, +26.7

NICS(1)$_{zz}$ values for the S_0, T_1, and Q_1 states were computed at PW91/IGLOIII//ωB97X-D/6–311+G(d,p).

Conclusions

Antiaromatic molecules, unless kinetically trapped, fused to aromatic frameworks, or stabilized by chemical modifications, often are short-lived and difficult to work with experimentally—they always find ways of escaping the state of being called "antiaromatic." Cyclobutadiene, cyclopentadienone, pentalene, and other cyclic, π-conjugated compounds, with formal [$4n$] ring π-electrons, easily dimerize to get rid of antiaromaticity. Upon irradiation, benzene rather isomerize to fulvene and the very strained benzvalene than stay [$4n + 2$] π-electron antiaromatic (49). We show here that many organic compounds that undergo ESPT are antiaromatic at their first ππ* states—and proton transfer provides the perfect escape route.

The term "antiaromaticity" (just 2 y past its 50th anniversary this year) (50) has evolved quickly from a concept that picks theoretical interest and invites synthetic challenges, to a poster child for many modern applications of chemistry. The relationship discussed here, between excited-state antiaromaticity and ESPT, is another celebration of the antiaromaticity concept. Recognizing the role of excited-state antiaromaticity in ESPT reactions has tremendous interpretive value for understanding the photochemistry of many organic and biological systems. We hope that the emphasized role of excited-state antiaromaticity in ESPT discussed here will open up opportunities, for applications of this useful class of reaction, and for harnessing the effects of light for tuning hydrogen bonds.

Methods

All geometries were optimized at (TD-)ωB97X-D/6–311+G(d,p) using the Gaussian16 program (see full reference in *SI Appendix*). Vibrational frequency analyses verified the nature of stationary points. Gas-phase tautomeric energies were computed at (TD-)ωB97X-D/6–311+G(d,p); results in implicit solvation and benchmark results against equation-of-motion coupled-cluster singles and doubles (EOM-CCSD)/6–311+G(d,p) data are included in *SI Appendix*, Tables S11 and S12. All gas-phase interaction energies (ΔE_{int}) and tautomerization energies (ΔE_T) include zero-point vibrational energy corrections. Dissected NICS(1)$_{zz}$ (40, 41)were computed at 1 Å above the 5- and 6-membered ring of all compounds and complexes considered and include only contributions from the out-of-plane (*zz*) tensor component perpendicular to the ring plane. All NICS(1)$_{zz}$ values were computed at the PW91/IGLOIII level. NICS(1)$_{zz}$ values for the S_1 states were approximated based on NICS calculations performed as open-shell triplet states using geometries optimized at the S_1 state. NICS(1)$_{zz}$ data for the S_2 state of *o*-salicylic acid was computed at complete active space self-consistent field (CASSCF)/6–311+G(d,p) (see results for S_0 and S_1 in *SI Appendix*,

Table S9). GIMIC (48) vectors for the S_0, T_1, and Q_1 states of the 2-$AP_{(A)}$ dimer and 2-$AP_{(Q)}$ dimer were evaluated at 1 Å above the rings with the magnetic field axis placed perpendicular to the ring plane. Based on the respective dimer geometries, difference plots of GIMIC, ΔGIMIC, were generated by differences of the computed ring current vectors of a 6-membered ring moiety with and without its hydrogen bonding partner. See *SI Appendix* for full methods.

ACKNOWLEDGMENTS. J.I.W. thanks the National Science Foundation (NSF) (CHE-1751370) and National Institute of General Medical Sciences (NIGMS) of the NIH (R35GM133548) for grant support, as well as computational resources provided by the uHPC cluster, managed by the University of Houston and acquired through support from the NSF (MRI-1531814). H.O. thanks the Swedish Research Council for grant support (2015-04538).

1. A. Weller, Quantitative untersuchungen der fluoreszenzumwandlung bei naphtholen. *Elektrochemie* **56**, 662–668 (1952).
2. A. Weller, Fast reactions of excited molecules. *Prog. React. Kinet.* **1**, 187–214 (1961).
3. K. K. Smith, K. J. Kaufmann, Solvent dependence of the nonradiative decay rate of methyl salicylate. *J. Phys. Chem.* **85**, 2895–2897 (1981).
4. S. Nagaoka, U. Nagashima, N. Ohta, M. Fujita, T. Takemura, Electronic-state dependence of intramolecular proton transfer of o-hydroxybenzaldehyde. *J. Phys. Chem.* **92**, 166–171 (1988).
5. S. Nagaoka, U. Nagashima, Intramolecular proton transfer in various electronic states of o-hydroxybenzaldehyde. *Chem. Phys.* **136**, 153–163 (1989).
6. J. Waluk, Hydrogen-bonding-induced phenomena in bifunctional hetero-azaaromatics. *Acc. Chem. Res.* **36**, 832–838 (2003).
7. C. al-Taylor, M. Ashraf el-Bayoumi, M. Kasha, Excited-state two-proton tautomerism in hydrogen-bonded n-heterocyclic base pairs. *Proc. Natl. Acad. Sci. U.S.A.* **63**, 253–260 (1969).
8. J. Sepiol, U. P. Wild, Excited-state double proton transfer in heterodimers of 1-azacarbazole. *Chem. Phys. Lett.* **93**, 204–207 (1982).
9. J. Waluk, S. J. Komorowski, J. Herbich, Excited-state double proton transfer in 1-azacarbazole-alcohol complexes. *J. Phys. Chem.* **90**, 3868–3871 (1986).
10. K. Inuzuka, A. Fujimoto, Electronic properties and ultraviolet absorption and fluorescence spectra of 2-pyridinamine. *Spectrochim. Acta* **42**, 929–937 (1986).
11. J. Konijnenberg, A. H. Huizer, C. A. G. O. Varma, A time-resolved study of the photoinduced tautomerization of 2-aminopyridine and derivatives within specific 1:1 complexes with carboxylic acids. *J. Chem. Soc. Faraday Trans. 2* **85**, 1539–1552 (1989).
12. H. Ishikawa, K. Iwata, H. Hamaguchi, Picosecond dynamics of stepwise double proton-transfer reaction in the excited state of the 2-aminopyridine/acetic acid system. *J. Phys. Chem. A* **106**, 2305–2312 (2002).
13. L. G. Arnaut, S. J. Formosinho, Excited-state proton transfer reactions I. Fundamentals and intermolecular reactions. *J. Photochem. Photobiol. A Chem.* **75**, 1–20 (1993).
14. P. K. Sengupta, M. Kasha, Excited-state proton-transfer spectroscopy of 3-hydroxyflavone and quercetin. *Chem. Phys. Lett.* **68**, 382–385 (1979).
15. G. J. Woolfe, P. J. Thistlethwaite, Direct observation of excited state intramolecular proton transfer kinetics in 3-hydroxyflavone. *J. Am. Chem. Soc.* **103**, 6916–6923 (1981).
16. M. Itoh, Y. Fujiwara, Transient absorption and two-step laser excitation fluorescence studies of photoisomerization in 2-(2-hydroxyphenyl)benzoxazole and 2-(2-hydroxyphenyl)benzothiazole. *J. Am. Chem. Soc.* **107**, 1561–1565 (1985).
17. M. L. Martinez, W. C. Cooper, P.-T. Chou, A novel excited-state intramolecular proton transfer molecule, 10-hydroxybenzo[h]quinoline. *Chem. Phys. Lett.* **193**, 151–154 (1992).
18. S. J. Formosinho, L. G. Arnaut, Excited-state proton transfer reactions II. Intramolecular reactions. *J. Photochem. Photobiol. A Chem.* **75**, 21–48 (1993).
19. J. E. Kwon, S. Y. Park, Advanced organic optoelectronic materials: Harnessing excited-state intramolecular proton transfer (ESIPT) process. *Adv. Mater.* **23**, 3615–3642 (2011).
20. A. J. Stasyuk, Y.-T. Chen, C.-L. Chen, P.-J. Wu, P.-T. Chou, A new class of N-H excited-state intramolecular proton transfer (ESIPT) molecules bearing localized zwitterionic tautomers. *Phys. Chem. Chem. Phys.* **18**, 24428–24436 (2016).
21. M. Forés, M. Duran, M. Solà, L. Adamowicz, Excited-state intramolecular proton transfer and rotamerism of 2-(2′-hydroxyvinyl)benzimidazole and 2-(2′-hydroxyphenyl)imidazole. *J. Phys. Chem. A* **103**, 4413–4420 (1999).
22. L. Gutiérrez-Arzaluz, F. Cortés-Guzmán, T. Rocha-Rinza, J. Peón, Ultrafast excited state hydrogen atom transfer in salicylideneaniline driven by changes in aromaticity. *Phys. Chem. Chem. Phys.* **17**, 31608–31612 (2015).
23. A. J. Stasyuk, P. Bultinck, D. T. Gryko, M. K. Cyrański, The effect of hydrogen bond strength on emission properties in 2-(2′-hydroxyphenyl)imidazo[1,2-a]pyridines. *Photochem. Photobiol. A Chemistry* **314**, 198–213 (2016).
24. N. Nishina, T. Mutai, J.-I. Aihara, Excited-state intramolecular proton transfer and global aromaticity. *J. Phys. Chem. A* **121**, 151–161 (2017).
25. N. C. Baird, Quantum organic photochemistry. II. Resonance and aromaticity in the lowest $^3\pi\pi^*$ state of cyclic hydrocarbons. *J. Am. Chem. Soc.* **94**, 4941–4948 (1972).
26. J.-I. Aihara, Aromaticity-based theory of pericyclic reactions. *Bull. Chem. Soc. Jpn.* **51**, 1788–1792 (1978).
27. V. Gogonea, P. R. Schleyer, P. R. Schreiner, Consequence of triplet aromaticity in 4n π-electron annulenes: Calculation of magnetic shieldings for open-shell species. *Angew. Chem. Int. Ed.* **37**, 1945–1948 (1998).
28. P. B. Karadakov, Ground- and excited-state aromaticity and antiaromaticity in benzene and cyclobutadiene. *J. Phys. Chem. A* **112**, 7303–7309 (2008).
29. F. Feixas, J. Vandenbussche, P. Bultinck, E. Matito, M. Solà, Electron delocalization and aromaticity in low-lying excited states of archetypal organic compounds. *Phys. Chem. Chem. Phys.* **13**, 20690–20703 (2011).
30. Y. M. Sung *et al.*, Reversal of Hückel (anti)aromaticity in the lowest triplet states of hexaphyrins and spectroscopic evidence for Baird's rule. *Nat. Chem.* **7**, 418–422 (2015).
31. J. Oh, Y. M. Sung, Y. Hong, D. Kim, Spectroscopic diagnosis of excited-state aromaticity: Capturing electronic structure and conformations upon aromaticity reversal. *Acc. Chem. Res.* **51**, 1349–1358 (2018).
32. M. Rosenberg, C. Dahlstrand, K. Kilså, H. Ottosson, Excited state aromaticity and antiaromaticity: Opportunities for photophysical and photochemical rationalizations. *Chem. Rev.* **114**, 5379–5425 (2014).
33. H. Ottosson, Organic photochemistry: Exciting excited-state aromaticity. *Nat. Chem.* **4**, 969–971 (2012).
34. R. Papadakis, H. Ottosson, The excited state antiaromatic benzene ring: A molecular Mr Hyde? *Chem. Soc. Rev.* **44**, 6472–6493 (2015).
35. M. Kasha, Proton-transfer spectroscopy. Perturbation of the tautomerization potential. *J. Chem. Soc. Faraday Trans. 2* **82**, 2379–2392 (1986).
36. P. S. Song, M. Sun, A. Koziolawa, J. Koziol, Phototautomerism of lumichromes and alloxazines. *J. Am. Chem. Soc.* **96**, 4319–4323 (1974).
37. J. D. Choi, R. D. Fugate, P.-S. Song, Nanosecond time-resolved fluorescence of phototautomeric lumichrome. *J. Am. Chem. Soc.* **102**, 5293–5297 (1980).
38. M. Itoh, T. Adachi, K. Tokumura, Time-resolved fluorescence and absorption spectra and two-step laser excitation fluorescence of the excited-state proton transfer in the methanol solution of 7-hydroxyquinoline. *J. Am. Chem. Soc.* **106**, 850–855 (1984).
39. C. Tanner, C. Manca, S. Leutwyler, Probing the threshold to H atom transfer along a hydrogen-bonded ammonia wire. *Science* **302**, 1736–1739 (2003).
40. Z. Chen, C. S. Wannere, C. Corminboeuf, R. Puchta, Pv. Schleyer, Nucleus-independent chemical shifts (NICS) as an aromaticity criterion. *Chem. Rev.* **105**, 3842–3888 (2005).
41. C. Corminboeuf, T. Heine, G. Seifert, P. R. Schleyer, J. Weber, Induced magnetic fields in aromatic [n]-annulenes—interpretation of NICS tensor components. *Phys. Chem. Chem. Phys.* **6**, 273–276 (2004).
42. B. J. Lampkin, Y. H. Nguyen, P. B. Karadakov, B. VanVeller, Demonstration of Baird's rule complementarity in the singlet state with implications for excited-state intramolecular proton transfer. *Phys. Chem. Chem. Phys.* **21**, 11608–11614 (2019).
43. P. B. Karadakov, P. Hearnshaw, K. E. Horner, Magnetic shielding, aromaticity, antiaromaticity, and bonding in the low-lying electronic states of benzene and cyclobutadiene. *J. Org. Chem.* **81**, 11346–11352 (2016).
44. S. Nagaoka *et al.*, Nodal-plane model of the excited-state intramolecular proton transfer of 2-(o-hydroxyaryl)benzazoles. *J. Photochem. Photobiol. A Chem.* **122**, 151–159 (1999).
45. M. T. Rogers, The electric moments of some derivatives of pyridine and quinoline. *J. Phys. Chem.* **60**, 125–126 (1956).
46. A. Weisstuch, A. C. Testa, Fluorescence study of aminopyridines. *J. Phys. Chem.* **72**, 1982–1987 (1968).
47. T. Schultz *et al.*, Efficient deactivation of a model base pair via excited-state hydrogen transfer. *Science* **306**, 1765–1768 (2004).
48. H. Fliegl, S. Taubert, O. Lehtonen, D. Sundholm, The gauge including magnetically induced current method. *Phys. Chem. Chem. Phys.* **13**, 20500–20518 (2011).
49. L. Kaplan, K. E. Wilzbach, Photolysis of benzene vapor. Benzvalene formation at wavelengths 2537-2370 A. *J. Am. Chem. Soc.* **90**, 3291–3292 (1968).
50. R. Breslow, J. Brown, J. J. Gajewski, Antiaromaticity of cyclopropenyl anions. *J. Am. Chem. Soc.* **89**, 4383–4390 (1967).